ELSEVIER

Journal of Power Sources 109 (2002) 301–307

JOURNAL OF POWER SOURCES

www.elsevier.com/locate/jpowsour

Luminescence in some lithiated transition metal oxide cathodes

P. Kalyani[a], R. Jagannathan[a,*], S. Gopukumar[a], Chung-Hsin Lu[b]

[a]*Central Electrochemical Research Institute, Karaikudi 630006, India*

[b]*Department of Chemical Engineering, National Taiwan University, Taipei 10617, Taiwan, ROC*

Received 12 October 2001; received in revised form 18 January 2002; accepted 24 January 2002

Abstract

Lithiated transition metal oxides such as $LiNiVO_4$, Li_2MnO_3 and $Li_{0.4}WO_3$ used as cathode materials in high density lithium-ion batteries, show intense optical absorption followed by fluorescence in the region of 2–4 eV. These optical transitions can tentatively be assigned to either transition metal to oxygen charge transfer type or Jahn-Teller type local distortion. For fluorescing samples ($LiNiVO_4$, Li_2MnO_3 and $Li_{0.4}WO_4$), photo-induced impedance (Bode plot) data show significant enhancement in impedance under low frequency range (~10 Hz). However, more important cathode materials such as $LiCoO_2$ and $LiMn_2O_4$ do not show either fluorescence or photo-induced impedance enhancement. The presence or absence of an optical transition in the cathode system may give some clues on the tendency for electrochemical fading.

Keywords: Luminescence; Bode plot; Electrochemical fading; Cathodes; Photo-induced impedance

1. Introduction

Lithiated transition metal oxides are useful as cathodes for lithium batteries because they offer a high cell voltage of 4 V combined with high capacity from a given amount of electrode material (ca. 120 mAh/g) [1]. Although $LiCoO_2$ has been the most successful cathode system in lithium-ion batteries, cost and toxicity considerations have led to the search for new alternatives having disparate chemical constituents and electrochemical properties. Mostly, these efforts have been centered around exploring various transition metal (TM) ions and their redox potential determined by the oxygen network surrounding TM ions. Using first principle calculations based on ultra-soft pseudo-potential method, Ceder et al. [2] have shown that it is theoretically (also experimentally) possible to realize cell voltages as high as 5.4 V. It has been further argued that, the electron exchange responsible for the Li-intercalation/de-intercalation voltage is determined mostly by the oxygen network. Also it has been experimentally demonstrated that most of cathode materials, exhibit pronounced fading properties after considerable electrochemical cycling, e.g. some of the Li-managanate based systems [3]. Structural studies on these electrochemically cycled materials have shown that there is considerable reduction in the structural symmetry of the cathode system [4]. The reduction in local symmetry around the TM ion has been visualized in terms of Jahn-Teller distortion. In the formidable task of exploring various cathode materials (having disparate chemical properties), a number of transition metal ions have been employed. However, in our opinion, the role of transition metal ions in explaining electrochemical properties has not received due consideration. To highlight this issue, we present and discuss the results of fluorescence and diffuse reflectance studies on the cathode materials. The cathode materials are divided into two classes, viz. (i) systems with non-centro-symmetric sites such as $LiNiVO_4$, Li_2MnO_3, and $Li_{0.4}WO_3$ systems and (ii) cubic systems such as $LiCoO_2$ and $LiMn_2O_4$ having perfect O_h symmetry for the TM ion. We believe the results of this investigation will add some new insights that may be complementary to the information already available in literature.

2. Material synthesis and characterization

In this investigation, all compounds investigated (except lithium tungstate) were prepared by combustion synthesis [5]. For the combustion synthesis, stoichiometric amounts of the respective nitrates were dissolved in minimum quantity of distilled water. To this homogeneous mixture, calculated amount of a fuel was added to provide sufficient heat energy for the completion of the reaction so that the target phase can be achieved. The mixture was first heated at 100 °C so as to be free from water content. The sticky mass was then fired at

* Corresponding author.
E-mail address: jags57_99@yahoo.com (R. Jagannathan).

0378-7753/02/$ – see front matter
PII: S0378-7753(02)00057-5

800 °C for 3 h to yield the final compound. In the case of $LiNiVO_4$ preparation, addition of calculated amount of ammonium vanadate and minimum quantity of ammonia solution (to facilitate the dissolution of ammonium vanadate) preceded the above heating schedule. The following equations represent the chemical reactions during the combustion process:

$$\begin{cases} LiNO_3 + Co(NO_3)_3 \rightarrow LiCoO_2 + \text{gases} \\ LiNO_3 + NH_4(VO_3) + Ni(NO_3)_2 \rightarrow LiNiVO_4 + \text{gases} \\ 2LiNO_3 + Mn(NO_3)_3 \rightarrow Li_2MnO_3 + \text{gases} \\ LiNO_3 + 2Mn(NO_3)_3 \rightarrow LiMn_2O_4 + \text{gases} \end{cases} \quad (q(\text{urea}),\ 800\,^{\circ}\text{C},\quad 2\,\text{mol} < q < 5\,\text{mol}) \tag{1}$$

The flow chart given in Fig. 1 explains the process of synthesizing crystalline compounds by combustion synthesis (except for the tungstate system).

Lithium tungstate ($Li_{0.4}WO_3$) was synthesized using lithium hydroxide and tungstic acid as starting materials. The starting materials were taken with the composition corresponding to Eq. (2), thoroughly homogenized, first heated at 400 °C for 6 h and then at 800 °C for 16 h. The resulting product, a light blue powder was found to be lithium tungstate.

$$0.4LiOH + H_3WO_4 \rightarrow Li_{0.4}WO_3 + H_2O \tag{2}$$

XRD powder patterns were recorded with the help of a JEOL-JDX 8030 X-ray diffractometer using nickel filtered CuKα radiation ($\lambda = 1.54186$ Å) in the 2θ range 10–80°. All the diffraction patterns were recorded at room temperature. The scan rate was 0.1°/s. The XRD patterns did not show any extra lines indicating the absence of noticeable impure phases. The diffraction peaks were indexed assuming cubic structure for $LiMn_2O_4$ ($Fd3m$) [6] and $LiNiVO_4$ ($Fd\bar{3}m$) [7], and rhombohedral ($R\bar{3}m$) for $LiCoO_2$ [8], monoclinic ($C2/m$) for Li_2MnO_3 [9], and hexagonal for $Li_{0.4}WO_3$ [10]. The data on crystallographic cell parameters have been refined using a least-squares fitting procedure. The least-squares refined lattice parameters listed in Table 1 are in good accord with standard values including standard JCPDS files reported in the literature. Fluorescence spectra were recorded using a Hitachi 650-10S fluorescence spectrophotometer equipped with a 150 W Xenon lamp and Hamamatsu R928 F photomultiplier. We measured the fluorescence spectra of the samples at various temperatures in the range of 15–300 K by loading the sample in to the cold finger of cryostat. Since the sample loading conditions are the same through out the temperature range studied, the fluorescence intensity measured for a given sample can be directly used to know temperature-dependent change in fluorescence intensity. Diffuse reflectance spectra were recorded with the help of Hitachi U-3400 double beam UV–VIS spectrophotometer using a high alumina pellet as the reference.

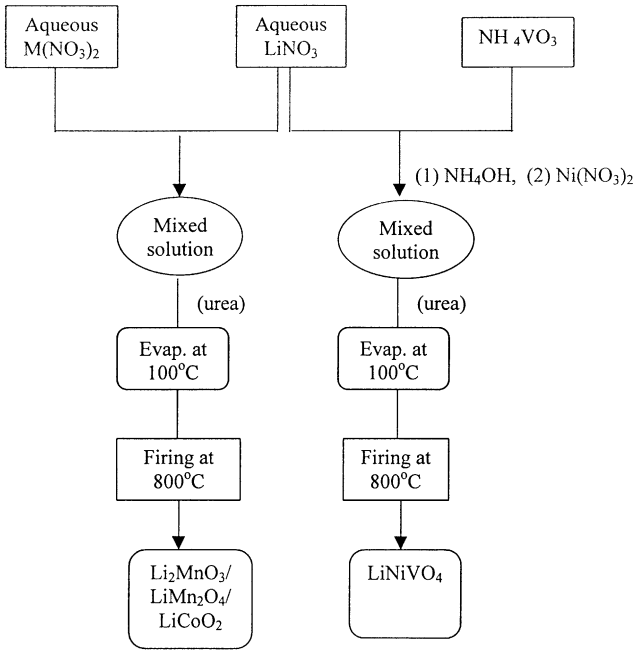

Fig. 1. Flow chart giving various steps involved in the combustion synthesis of cathode materials.

Table 1
Refined cell parameters of lithiated compounds using least-squares fitting method

Compound	Space group	Crystal structure	Cell parameters		JCPDS file no. (for reference)
			a (Å)	c (Å)	
$LiMn_2O_4$	$Fd3m$	Cubic	8.24 (8.23)	–	18-0736
$LiCoO_2$	$R\bar{3}m$	Rhombohedral	2.835 (2.816)	14.06 (14.05)	16-0427
Li_2MnO_3	$C2/m$	Monoclinic	–	–	18-0737
$LiNiVO_4$	$Fd\bar{3}m$	Cubic	8.19 (8.22)	–	38-1395
$Li_{0.4}WO_3$[a]		Hexagonal	7.314	7.542	–

The values given in the parenthesis indicate the standard values.
[a] Indexed assuming hexagonal settings.

Impedance measurements (two probe) were carried out using EG&G instrument (Model no. 5210, Princeton Applied Research, USA) interfaced with a personal computer. Cathode materials were made into pellets of 5 mm thickness and 18 mm diameter using a hydraulic press (load was 8 kg/cm^2). In order to make effective electrical contact, silver paste was coated on both sides of the pellets and copper leads from the sides were taken with the leads in contact with the pellets. After connecting the two probes of the instruments to the two leads of the pellets, impedance data were collected for the frequency range 0.1 Hz to 10 kHz by imposing an ac voltage of amplitude 5 mV (rms). Photo-induced impedance measurements were made using ultra-violet lamps with suitable filters to give UV radiation of either 254 or 365 nm and a rated power of 20 W. The UV lamp was held as close to the pellet as (~2 cm) possible. An activation time of 2 min was maintained for all the pellets before commencing the experiment. During the measurements, interference from extraneous light was taken care of by handling the samples in a black container with a window for the UV light to pass through.

3. Results and discussion

3.1. Optical transitions in lithiated cathodes

In Table 2 and Figs. 2 and 3, we present the optical data concerning fluorescence and UV–VIS absorption studies on the cathode materials investigated. From the fluorescence spectra given in Fig. 2, it is obvious that for excitation in the UV region (λ_{exc} = 290–450 nm) $LiNiVO_4$, Li_2MnO_3 and $Li_{0.4}WO_3$ samples give characteristic fluorescence in the visible region with emission maxima at 560, 425 and 450 nm, respectively. Furthermore, it has been found that the low temperature fluorescence spectra of $LiNiVO_4$ sample

Table 2
Structural and spectroscopic details of lithiated transition metal oxide cathodes

Cathode material	Theoretical cell voltage (V)	Transition metal ion	Local symmetry	Charge transfer species	Selection rule (symmetry)	Optical absorption/ fluorescence observed
$LiMn_2O_4$	4	Mn^{3+}	O_h[a]	Mn–O	Forbidden	No
		Mn^{4+}	O_h[a]		(Allowed[a])	
$LiCoO_2$	4	Co^{3+}	O_h	Co–O	Forbidden	No
Li_2MnO_3	3	Mn^{4+}	C_2	Mn–O	Allowed	Yes
$LiNiVO_4$	4.8	Ni^{2+}	O_h	Ni–O	Forbidden	No
		V^{5+}	T_d	V–O	Allowed	Yes
$Li_{0.4}WO_3$	1.5	W^{5+}		W–O	Allowed	Yes

[a] Lower symmetry possible due to Jahn-Teller distortion.

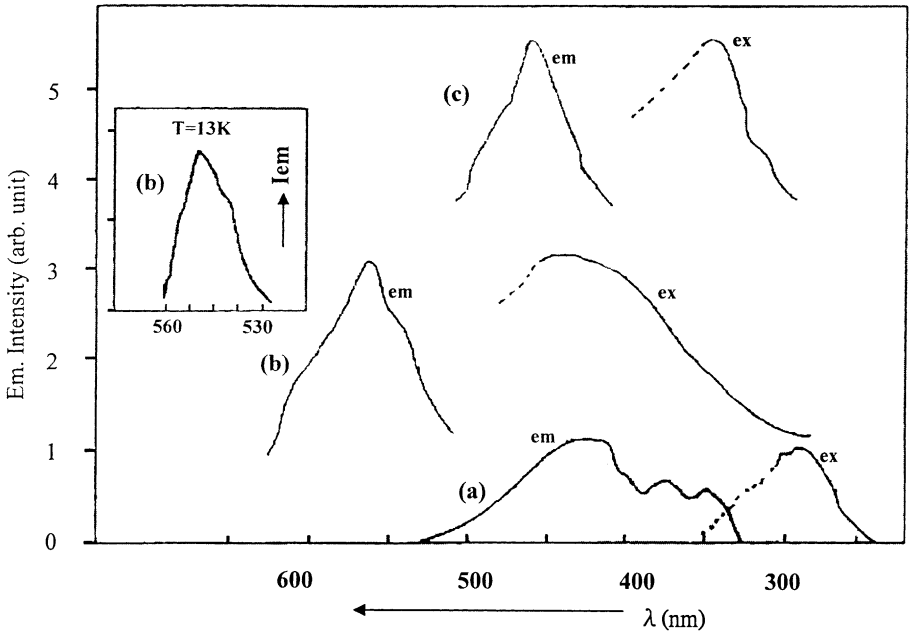

Fig. 2. Fluorescence (emission and excitation at T = 300 K) spectra of: (a) Li_2MnO_3, (b) $LiNiVO_4$, and (c) $Li_{0.4}WO_3$. Emission of spectrum of $LiNiVO_4$ at T = 13 K (inset).

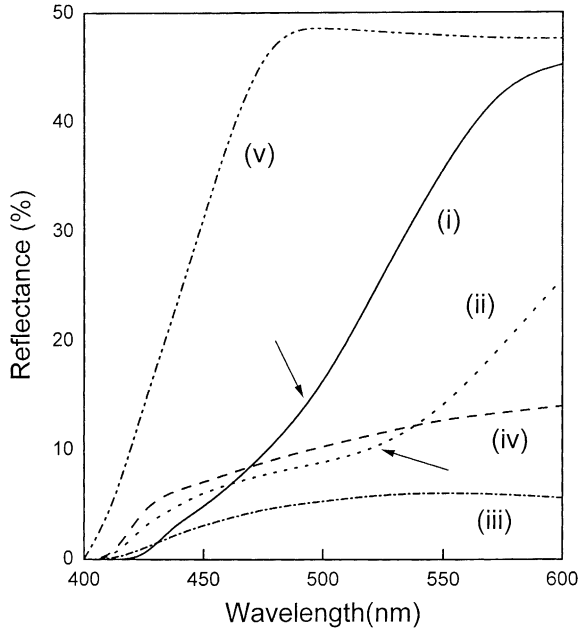

Fig. 3. Diffuse reflectance spectra (at $T = 300$ K) of various cathode materials as indicated: (i) $LiNiVO_4$, (ii) Li_2MnO_3, (iii) $LiMn_2O_4$, (iv) $LiCoO_2$, and (v) $Li_{0.4}WO_3$.

(Fig. 2, inset) did not show any spectacular change in fluorescence intensity implying absence of any thermal quenching of fluorescence at room temperature. However, it can be seen from the spectra that there is considerable narrowing of the bandwidth accompanied by a slight blue-shift in the emission band. Narrowing of the emission band on lowering the sample temperature can be attributed to minimization of contribution from phonon side-bands due to lattice–phonon interaction related to the luminescent center versus lattice.

On the other hand, $LiCoO_2$ and $LiMn_2O_4$ systems do not show any fluorescence in the region we studied (200–800 nm). From the UV–VIS reflectance spectra given in Fig. 3, the presence of intense absorption around 520 nm is obvious in Li_2MnO_3 system, while for the case of $LiNiVO_4$, a weak absorption around 490 nm can be observed. For the case of $LiCoO_2$ and $LiMn_2O_4$ samples, there are no such features observable in the reflectance spectra. Also it can be seen that in the case of Li-tungstate system, an intense absorption sets in around 450 nm.

Since most of these optical transitions are in the region of 2–4 eV (350–600 nm), these can be categorically assigned to electronic transitions involving the TM ion(s) and oxygen ions surrounding the TM ion(s). We outrightly reject the possibility that these transitions may originate from species involving Li–oxygen (Li–O) network. This is because, from the first principle calculation, we have that the hypothetical intercalation voltage (for Li in conjunction with a non-transition element such as Al as the other cation) works out to be as high as 5.4 V [2] (which means an energy around 5.4 eV for any electronic transition to be associated with this process when in circuit). Furthermore, as far as we are aware, there are no reports on such optical transitions involving these species.

3.2. Photo-induced impedance data

In order to identify the origin and nature of the electronic transitions observed in the visible region, we measured the impedance spectra for these samples both under UV exposure (254 and 365 nm radiation) and without UV exposure. We consider frequency versus impedance Bode plot can bring about more information on various electronic transitions, in particular, various electronic transitions operating with different time constants. For the $LiNiVO_4$ sample, once it was exposed to UV (both 254 and 365 nm radiation), we observed a spectacular change (to the extent of one order enhancement) in the impedance values in the low frequency region (10–100 Hz, Fig. 4). For the $LiNiVO_4$ system, there is an obvious enhancement by nearly one order in the impedance value in the low frequency region. This may be explained by considering some photo-induced electron transfer process between the transition metal ion (V^{5+}) and the oxygen network surrounding it.

However, for the case of Li_2MnO_3 system, the impedance values are highly scattered, irrespective of whether the sample was being exposed to UV radiation or not. This makes it less obvious to know if there is any UV-induced impedance enhancement for the Li_2MnO_3 system. Still from Fig. 4, curve (d) corresponding to the Li_2MnO_3 system, a slight enhancement in the impedance value in the low frequency range can be observed both for the case of with and without UV exposure. On the other hand, for $LiCoO_2$ and $LiMn_2O_4$ systems, there was no such light dependent impedance enhancement observed. However, for reasons of brevity, we present in Fig. 4, the impedance data related to $LiMn_2O_4$ system only as an illustrative comparison.

3.3. Luminescence from charge transfer or Jahn-Teller distortion type transitions

We consider that a suitable correlation between the above phenomena can bring about a lot of information concerning the cathode materials. This can of relevance in explaining some of the electrochemical properties. In order to explain the presence or absence of the optical transitions in these materials, a brief description on the structural details of these systems is imperative.

From Table 1, we have that $LiMn_2O_4$ has a cubic spinel structure with *Fd*3*m* space group symmetry. Here, the Mn ion exists in two valencies, viz. 4+ and 3+ and hence, the average valency works out to be 3.5. The Mn ion occurs in sites with perfect O_h symmetry [6]. For the $LiCoO_2$ system, a rhombohedral structure with $R\bar{3}m$ symmetry has been reported and further the point group symmetry for Co^{3+} ion is reported to be an O_h symmetry [8]. In the case of $LiCoO_2$ system, there seems to be some structural incompatibility problem for the cubic O_h site (asking for a 4-fold

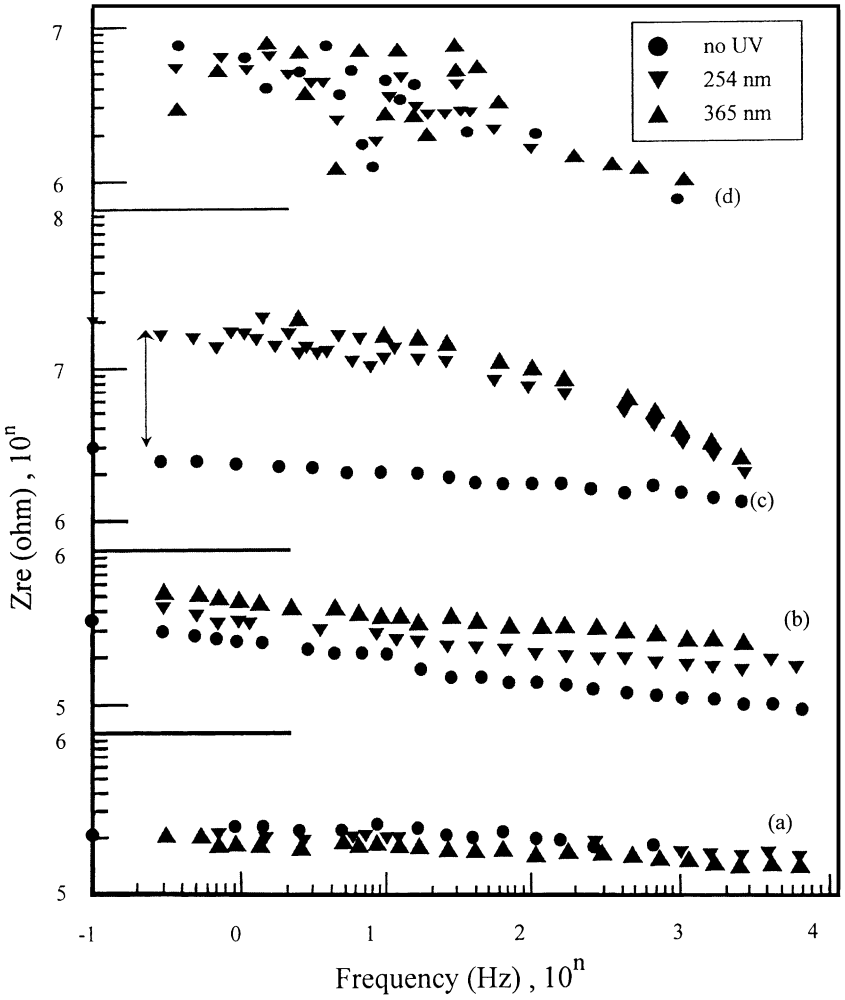

Fig. 4. Bode plots of various cathode materials with and without UV exposure as indicated: (a) $LiMn_2O_4$, (b) $Li_{0.4}WO_3$, (c) $LiNiVO_4$, and (d) Li_2MnO_3.

rotation axis) to occupy a rhombohedral $R\bar{3}m$ crystal symmetry (having a maximum of 3-fold rotation axis). Notwithstanding this, for the Co^{3+} ion with $3d^6$ configuration (corresponding to the lowest state ^3P) in a centro-symmetric O_h site is unfavorable to show any intra-configurational d–d transitions. For this reason, it is not expected to show any optical transitions.

An optical transition is possible if there is severe break down of restrictions in selection rules. On the other hand, for the case of $LiMn_2O_4$, where the Mn^{3+} and Mn^{4+} ions (corresponding to $3d^4$ and $3d^3$ electron configurations) sit in a site with perfect O_h symmetry. Presence of an inversion center in the cubic site, again precludes all possibilities for observing any optical transitions in the $LiMn_2O_4$ system.

Now let us turn to cathode materials which show optical transitions (both UV–VIS absorption and fluorescence). The case of Li_2MnO_3 is quite clear and straight forward in that for the TM ion (Mn) in the monoclinic Li_2MnO_3 can have at the most a non-centro-symmetric C_2 symmetry. This can considerably split the d-level of the Mn ion (to remove orbital degeneracy by Jahn-Teller distortion) so that optical transition(s) between some of the states would become possible. The cubic ($LiMn_2O_4$) to monoclinic (Li_2MnO_3) distortion is obvious from the splitting in the (1 3 5) and (0 6 0) XRD lines. This splitting corresponds to cation disorder leading to lowering of symmetry in the Li–Mn–O network [9].

$LiNiVO_4$ and $Li_{0.4}WO_3$ systems altogether belong to a different category. $LiNiVO_4$ adopts a cubic $Fd\bar{3}m$ inverse spinel structure with Ni^{2+} ($3d^8$) and V^{5+} ($3d^0$) in cationic sites, respectively with an octahedral O_h and tetrahedral T_d symmetries. Hence, this imposes restriction for the Ni^{2+} ion to show an optical transition while no such restriction applies to the V^{5+} ion. The $LiNiVO_4$ system shows an intense emission band around 560 nm with the excitation maximum at 430 nm (Fig. 2). This corresponds to a Stoke's shift of about 6100 cm^{-1} which compares well with the value of 8000 cm^{-1} known for YVO_4 system—a well known industrial phosphor [11,12]. In the YVO_4 system (usually doped with Eu^{3+} for luminescent lighting applications), the *ortho*-vanadate $(VO_4)^{3-}$ group gives the characteristic fluorescence around 450 nm due to V^{5+} ($3d^0$)–O^{2-} ($2p^6$) ligand

to metal $^1A_1 \rightarrow {}^1T_1$ ($3d^{x+1} \leftarrow 2p^{-1}$)) charge transfer transition. This host emission is known to undergo significant concentration quenching while thermal quenching effect (decrease in fluorescence intensity with temperature) is absent [13]. In the same fashion, the $LiNiVO_4$ system also did not show any thermal quenching effects as we did not observe any substantial enhancement in fluorescence intensity when the temperature of the sample was lowered down to 13 K (Fig. 2, inset). Further we believe that in the case of $LiNiVO_4$ system, $(VO_4)^{3-}$ concentration may be considerably lower than the critical limit required to observe quenching effects. Hence, for the case of $LiNiVO_4$, we are inclined to assign the fluorescence observed to V–O charge transfer band. Alternatively, there exists one more possibility that this could be due to an intra-ion p–d transition of V^{5+} [14]. In view of the experimental limitations, we are unable to confirm this possibility.

The case of $Li_{0.4}WO_3$, a new entrant as a potential cathode material, is quite simple and direct. Here, the defect centers in $(WO_3)^{2-}$ group (in particular, the oxygen defects) are active optical centers showing fluorescence in the same fashion as scheelite type calcium tungstate ($CaWO_4$), another celebrated phosphor system [11] used in image-intensifier screens for radiography. Again the fluorescence features in this system can be explained on the same basis as used for the vanadate system.

Apart from the discussion based on the structural and optical data obtained, we would like to raise the following points which in our opinion are pertinent to have some insight on the cell voltage, the electrochemical cyclability and fading properties of the cathode material applied in the battery system.

(i) For $LiNiVO_4$ as the cathode, the cell system is unique in that it offers a very high cell voltage as high as 4.8 V. It is claimed by Ceder et al. [2] that in the Li-cathode system, the electron density is localized around oxygens rather than the Li-ion itself. It is common knowledge from the electronegativity concept that the Li-ion is more ionic than any of the transition metal ions. Furthermore, between V^{5+} and Ni^{2+}, the former is in its highest valence state while the latter is in its lowest valence state. This would imply an increased propensity to form a redox couple between themselves via the oxygen network so that the electron exchange will be limited between TM and O^{2-} ions resulting in higher cell voltage.

(ii) Li:TM ion ratio in particular Li:Mn ratio appears to be critical to determine the optical transition.

(iii) Sun and Jeon [15] have recently established that it is possible to prepare a new system based on sulfur-doped spinel type $LiAl_{0.24}Mn_{1.76}O_{3.98}S_{0.02}$ oxysulfide cathode material showing remarkable structural integrity during electrochemical cycling, i.e. better electrochemical cyclability. This has been attributed to overcoming Jahn-Teller type cubic–tetragonal structural distortion by adopting a special method of synthesis for the cathode material.

4. Concluding remarks

Investigations based on optical transitions in several lithiated transition metal cathodes have enabled us to classify these materials into two classes, viz. one which show optical transitions (absorption followed by fluorescence) and others that do not show such transitions. The cathode materials such as $LiNiVO_4$ and Li_2MnO_3 (in non-centro symmetric sites) are quite favorable to show optical transitions that are either d–d type or charge transfer type, while the latter category of materials such as $LiCoO_2$, $LiMn_2O_4$ and its related systems present in sites having inversion-symmetry (corresponding to O_h site symmetry) are not expected to show any optical transitions. It is pertinent to consider reports mentioning that there is no structural distortion for the electrochemically cycled $LiCoO_2$, while there is considerable structural distortion in the first category of materials such as $LiNiVO_4$ and Li_2MnO_3 showing significant electrochemical fading. Although we are not able to adequately explain the presence or absence of photo-induced impedance enhancement, we believe that this would constitute an important topic for research for extensive studies in future. Furthermore, some of the cathode material systems such as $LiNiVO_4$ upon UV exposure shows some enhancement in impedance value in the low frequency region. Based on these results, we propose that fluorescence technique coupled with photo-induced impedance studies can be used as a reliable tool to distinguish between various cathode materials to determine whether they are prone to electrochemical fading or not.

Acknowledgements

We are very grateful to the referees for the valuable suggestions. Our sincere thanks to Huang Yung Hsiang and Hong Hsin-Cheng for the helps received in drawing figures.

References

[1] T. Ohzuku, in: G. Pistoia (Ed.), Lithium Batteries, Elsevier, New York, 1994 (Chapter 6).
[2] G. Ceder, Y.M. Chiang, D.R. Sadoway, M.K. Aydinol, Y.I. Jang, B. Huang, Nature 392 (1998) 694.
[3] M.M. Thackeray, A. de Kack, M.H. Rossouw, D. Liles, R. Bittihn, D. Hoge, J. Electrochem. Soc. 139 (1992) 363.
[4] M.M. Thackeray, W.I.F. David, P.G. Bruce, J.B. Goodenough, Mater. Res. Bull. 18 (1982) 461.
[5] S.S. Manohar, K.C. Patil, J. Am. Ceram. Soc. 75 (1994) 3832.
[6] B. Scrosati, J. Electrochem. Soc. 139 (1992) 2776.
[7] G.T.K. Fey, W. Li, J.R. Dahn, J. Electrochem. Soc. 14 (1994) 2279.

[8] K. Mizushima, P.C. Jones, P.J. Wiseman, J.B. Goodenough, Mater. Res. Bull. 15 (1980) 783.
[9] M.H. Rossouw, M.M. Thackeray, Mater. Res. Bull. 26 (1991) 463.
[10] P.G. Dickens, A.C. Halliwell, D.J. Murphy, M.S. Wittingham, J. Electroanal. Chem. 71 (1971) 794.
[11] R.K. Datta, Trans. Metall. Soc. AIME 239 (1967) 355.
[12] K.H. Butler, Fluorescent Lamp Phosphors, The Pennsylvania State University Press, University Park, USA, 1980, p. 288.
[13] G. Blasse, Philips Res. Rep. 23 (1968) 344.
[14] D.S. McLure, in: F. Seitz, D. Turnbull (Eds.), Solid State Physics, Vol. 9, Academic Press, New York, 1959, p. 442.
[15] Y.K. Sun, Y.S. Jeon, J. Mater. Chem. 9 (1999) 3147.